Journal of Affective Disorders 374 (2025) 312–322

Contents lists available at ScienceDirect

Journal of Affective Disorders

journal homepage: www.elsevier.com/locate/jad

Research paper

Electroconvulsive therapy modulates brain functional stability in patients with major depressive disorder

Dongpeng Wu [a,c,1], Yue Yu [a,c,1], Hongping Wang [b,1], Jiahua Zhang [a,e,1], Jingyi You [a], Yiao Kai [g], Yue Zhao [a], Yue Wu [c], Kai Wang [a,d,e,f], Yanghua Tian [a,b,c,*]

[a] Department of Neurology, The First Affiliated Hospital of Anhui Medical University, 218 Jixi Road, Anhui Province, Hefei 230022, China
[b] Department of Neurology, The Second Affiliated Hospital of Anhui Medical University, Hefei 230601, China
[c] Department of Psychology and Sleep Medicine, The Second Affiliated Hospital of Anhui Medical University, Hefei 230601, China
[d] Anhui Province Key Laboratory of Cognition and Neuropsychiatric Disorders, 230022 Hefei, China
[e] School of Mental Health and Psychological Sciences, Anhui Medical University, 230022 Hefei, China
[f] Collaborative Innovation Center of Neuropsychiatric Disorders and Mental Health, 230022 Hefei, China
[g] Department of Anatomy, Anhui Medical University, Hefei 230032, Anhui, China

ARTICLE INFO

Keywords:
Functional stability
Major depressive disorder
Electroconvulsive therapy
Resting-state functional MRI

ABSTRACT

Background: Electroconvulsive therapy (ECT) is an effective treatment for patients with major depressive disorder (MDD), but the underlying neuromodulatory mechanisms remain largely unknown. Functional stability represents a newly developed method based on the dynamic functional connectivity framework. This study aimed to explore ECT-evoked changes in functional stability and their relationship with clinical outcomes.

Methods: We collected longitudinal resting-state fMRI data from 58 MDD patients (39 of whom experienced remission after ECT, and 19 did not, referred to as remitters and non-remitters, respectively) and 42 age- and sex-matched healthy controls. We utilized voxel-level whole-brain functional stability analysis to examine the neural effects of ECT in MDD patients.

Results: After ECT, MDD patients showed increased functional stability in the bilateral middle frontal gyrus, orbital part, and bilateral angular gyrus as well as decreased functional stability in the right fusiform gyrus. Additionally, the subgroup analysis revealed that functional stability of the right hippocampus significantly decreased in remitters yet significantly increased in non-remitters after ECT.

Conclusions: Our data demonstrated the modulatory effect of ECT on brain functional stability in MDD patients and further revealed the differences in this modulation between patients with and without clinical remission, highlighting the potential usefulness of functional stability as a prognostic biomarker for monitoring ECT efficacy and stratifying MDD patients to optimize treatment strategies.

1. Introduction

Major depressive disorder (MDD) is a prevalent mental illness that is characterized by vegetative symptoms, anhedonia, and a depressed mood (Otte et al., 2016). Electroconvulsive therapy (ECT) is a neuromodulation therapy for depression, during which electrodes are placed on the surface of the skull to stimulate an electric current, triggering epileptiform seizures to achieve specific therapeutic effects (Stippl et al., 2020). ECT can quickly and effectively relieve depression. A recent meta-analysis found that the response rate of ECT was 70 % for non-treatment-resistant depression, and 58 % for treatment-resistant depression (Haq et al., 2015). Despite the widespread clinical use of ECT, its neuromodulatory mechanisms remain poorly understood. Elucidating the underlying neurobiological processes by which ECT ameliorates MDD may optimize therapeutic strategies and enhance our understanding of the pathophysiology of this disease.

Resting-state functional magnetic resonance imaging (rs-fMRI) is a non-invasive neuroimaging technique for probing whole-brain spontaneous activity using blood oxygen level-dependent (BOLD) contrast and enables the study of sophisticated neural processes involving brain

* Corresponding author at: Department of Neurology, The First Affiliated Hospital of Anhui Medical University, 218 Jixi Road, Anhui Province, Hefei 230022, China.
E-mail address: ayfytyh@126.com (Y. Tian).
[1] These authors contributed equally to this work.

https://doi.org/10.1016/j.jad.2025.01.066
Received 28 September 2024; Received in revised form 4 January 2025; Accepted 13 January 2025
Available online 14 January 2025

functional integration and segregation (Barkhof et al., 2014).

Using rs-fMRI, our previous studies demonstrated that ECT led to changes in brain entropy (Fan et al., 2024) and nodal degree (Wu et al., 2022), as well as alterations in the intrinsic functional network topological architecture (Li et al., 2022) and the default mode network (Li et al., 2023). These findings partially reveal how ECT influences the brain's local and network-level properties. Resting-state functional connectivity (RSFC) is a commonly used fMRI measure, defined as the temporal coherence of low-frequency BOLD signal fluctuations across separated brain regions (Biswal et al., 1995; Fox and Greicius, 2010). This method has been widely applied to the study of the neuropathology of MDD and the neural effects of ECT treatment, such as exploring disease-related neurobiological differences in a cross-sectional manner (Kaiser et al., 2015; Mulders et al., 2015), investigating ECT-modulated changes in functional connectivity within large-scale functional networks (Pang et al., 2022; Wang et al., 2020), and examining the impact of intracranial electric field on ECT treatment outcomes through functional network connectivity (Fu et al., 2023).

Traditionally, most previous studies on functional connectivity have relied on static analytic methods, which assume that connectivity patterns remain consistent over time. However, there is emerging evidence that the brain is not a static system, and time-varying profiles of functional connectivity are evident across a broad range of task states and during periods of unconstrained rest (Chang and Glover, 2010). Thus, conventional static functional connectivity cannot capture the exact nature of spontaneous brain activity (Hutchison et al., 2013; Preti et al., 2017). Dynamic functional connectivity approaches may open new avenues for explaining brain function at different time scales, thereby potentially providing different but complementary information on disease mechanisms (Filippi et al., 2019). Under such circumstances, an increasing body of research has begun to exploit the rich temporal information contained within dynamic connectivity and has achieved significant success in revealing abnormalities in brain functional dynamics in patients with MDD (Chen et al., 2022; Demirtaş et al., 2016; Pang et al., 2018; Sendi et al., 2021). As ECT represents an effective neuromodulation approach for treating MDD, it is appealing to ask whether ECT can normalize or compensate for these brain dynamic functional abnormalities. Clarifying this issue may have implications for future ECT research and for achieving a deeper understanding of the neural effects of ECT that may ultimately inform clinical practice.

Although the brain dynamically integrates, coordinates, and responds to internal and external stimuli, maintaining a stable and consistent representation of information over time is equally essential for human behavior and cognition (Dehaene et al., 2017). Based on the dynamic functional connectivity framework, Li and colleagues proposed a voxel-wise functional stability measurement (Li et al., 2020). Functional stability can assess the concordance of dynamic functional connectivity of a voxel across time. A lower stability value indicates the ability to quickly and frequently switch between different brain states, whereas a higher stability value indicates that its dynamic functional architecture configuration is more constant and stable over time. Compared with traditional dynamic measures, such as the frequently used connection-wise variability (e.g., standard deviation) and connectivity states (e.g., states' temporal occurrences and dwell time, and between-state transition frequency), functional stability has its unique advantages. First, from the perspective of brain's functional architecture stability, functional stability characterizes temporal interval properties of dynamic functional connectivity, while connection-wise variability reflects variance of dynamic connectivity across time and connectivity states represent recurring whole-brain patterns of connectivity. Second, since functional stability is calculated at the voxel level, it has better spatial resolution than connection-wise variability at the connection level and connectivity states at the whole-brain level. Of more importance, recent cross-sectional and longitudinal studies have used this approach to explore brain dynamic functional abnormalities in many psychiatric disorders (Zhu et al., 2020) [PMID: 34217754]. However, there have been no attempts to use functional stability methods to detect brain functional changes evoked by ECT in MDD patients.

The current retrospective study aimed to explore the underlying neural mechanisms whereby ECT exerts its antidepressant effects, by analyzing brain functional stability derived from longitudinal rs-fMRI data of 58 MDD patients who underwent a standardized bifrontal ECT protocol. Specifically, we first investigated the modulatory effects of ECT on brain functional stability in MDD patients. Subsequently, we divided the patients into remitters and non-remitters to explore group differences in functional stability. We hypothesized that: (i) compared to healthy controls (HCs), MDD patients would exhibit abnormal functional stability, which can be modulated by ECT; (ii) ECT would have differential neural effects for the remitter and non-remitter groups.

2. Materials and methods

2.1. Participants

This study received approval from the Anhui Medical University Ethics Committee (study number: 20140072), and written informed consent was obtained from each participant. The inclusion criteria for participants were as follows: (1) All recruited patients had a clinical diagnosis of MDD, specifically categorized as either first-episode or chronic MDD; (2) an age range of 18 to 60 years; (3) absence of comorbid anxiety disorders, bipolar I or II disorder, schizophrenia, delusional disorder, and Axis II disorders as assessed by the Structured Clinical Interview for the Diagnostic and Statistical Manual of Mental Disorders, Fifth Edition (DSM-5) (SCID); (4) no history of neurologic or neurodegenerative disorders, such as head injury, epilepsy, or Alzheimer's disease; (5) no life-threatening somatic illnesses; (6) no ECT treatment within one year preceding the study; and (7) not currently pregnant. A total of 58 patients diagnosed with MDD and undergoing ECT were recruited from the Anhui Mental Health Center in Hefei, China. The diagnoses were confirmed by two trained psychiatrists by the criteria outlined in the DSM-5. Additionally, we recruited 42 age- and sex-matched HCs who had no current or past diagnosis of depression and had not undergone ECT, while the remaining inclusion criteria were the same as those applied to patients with MDD.

Clinical assessments and MRI scans for MDD were conducted at two distinct time points: 1) 12–72 h before the initial electroconvulsive therapy (pre-ECT), and 2) 72 h following the final ECT session (post-ECT). HCs underwent MRI scans twice, corresponding to the MDD procedures (initial scan: HC-scan1, follow-up scan: HC-scan2). The interval between the two scan sessions was 20.62 ± 2.63 days for HCs and 21.24 ± 6.74 days for MDD patients, with no significant difference in the scan intervals between the groups ($p = 0.639$). All participants were assessed using the 17-item Hamilton Rating Scale for Depression (HRSD) to evaluate the severity of depressive symptoms (Hamilton, 1967). The demographic information of MDD patients and HCs is shown in Table 1.

2.2. ECT procedures

All patients received a modified bifrontal ECT protocol delivered using a Thymatron System IV Integrated ECT (Somatics, Lake Bluff, IL, USA) at AMHC. The patient first underwent a pre-operative routine examination to rule out serious organ dysfunction, electrolyte disturbance, and other contraindications. Before ECT, patients were asked to fast from water for 8–12 h and stop anticonvulsant drugs such as benzodiazepines and lithium salts. Propofol (1.4 mg/kg) was used to induce general anesthesia, atropine (0.5 mg/kg) to suppress glandular secretion, succinylcholine (0.5 mg/kg) to induce muscle relaxation, dental pads were placed to prevent tongue bites, and respiratory support and EEG monitoring were performed. Regarding the ECT protocol, the initial energy percentage was established based on the individual's age (e.g., 50 % for a 50-year-old patient), and the stimulation intensity was systematically fine-tuned in increments of 5 % of the maximum charge

Table 1
Demographic and clinical measurements of MDD patients and healthy controls.

Characteristic	MDD (n = 58)	HC (n = 42)	Statistics	p-Value
Age (years)	38.62 ± 12.07	35.00 ± 11.61	$t = 1.504$[a]	0.136
Gender (male/female)	15/43	8/34	$\chi^2 = 0.639$[b]	0.424
Scan interval (days)	21.24 ± 6.74	20.62 ± 2.63	$t = 0.639$[a]	0.525
ECT sessions (n)	8(8,9.75)	NA	NA	NA
Illness duration (months)	24(6120)	NA	NA	NA
Episodes (first/recurrence, n)	22/36	NA	NA	NA
HRSD scores			$F = 207.01$[c]	<0.001
Baseline	23.03 ± 5.82	1.60 ± 1.75	$t = 21.45$[a]	<0.001
After ECT	7.07 ± 6.03	1.21 ± 1.88	$t = 6.33$[a]	<0.001

Note: Values are shown as the mean value ± standard deviation median (Q1, Q3). Abbreviations: MDD, major depressive disorder; HC, healthy control; NA, not applicable; ECT, electroconvulsive therapy; HRSD, Hamilton rating scale of depression.
[a] Two-sample t-tests.
[b] Pearson chi-squared test.
[c] Linear mixed effects model.

(approximately 1000 millicoulombs) until observable seizure activity was elicited. The whole seizure was recorded by connecting EEG. The initial three sessions were administered on consecutive days, followed by subsequent sessions held every alternate day, inclusive of breaks over the weekends, until patients achieved symptom remission. The total number of ECT treatments is 6–12 times for 2–3 weeks (Wang et al., 2019; Wei et al., 2014). There were no alterations to the medication regimen during the administration of ECT.

2.3. Imaging acquisition

MRI scans were acquired utilizing a 3.0-Tesla MR system (Discovery GE750; GE Healthcare, Buckinghamshire, UK) equipped with 8-channel head coil at the University of Science and Technology of China (USTC). Earplugs were employed to attenuate scanner noise, while snug yet comfortable foam padding was employed to mitigate head motion. Throughout the scanning procedure, participants received instructions to maintain closed eyes, a state of relaxation without drifting into sleep, absence of directed thinking, and minimal physical movement. The functional images composed of 217 echo-planar imaging (EPI) volumes (TR = 2400 ms; TE = 30 ms; flip angle = 90°; matrix size = 64 × 64, field of view = 192 × 192 mm^2; slice thickness = 3 mm; 46 continuous slices; voxel size = 3 × 3 × 3 mm^3) and T1 images with 188 slices were acquired (TR = 8.16 ms; TE = 3.18 ms; flip angle = 12; field of view = 256 × 256 mm^2; slice thickness = 1 mm; voxel size = 1 × 1 × 1 mm^3). Throughout and following the scanning procedure, we inquired with the participants to verify whether any of them had fallen asleep, ensuring that none had indeed done so. A visual inspection of all MRI images was conducted to ascertain the absence of any observable artifacts.

2.4. fMRI data preprocessing

Resting-state BOLD data were preprocessed using Statistical Parametric Mapping (SPM12, http://www.fil.ion.ucl.ac.uk/spm) and Data Processing & Analysis for Brain Imaging (DPABI, http://rfmri.org/dpabi) (Yan et al., 2016). The first 10 volumes for each participant were discarded to allow the signal to reach equilibrium and the participants to adapt to the scanning noise. The remaining volumes were corrected for the acquisition time delay between slices. Then, realignment was performed to correct the motion between time points. Head motion parameters were computed by estimating the translation in each direction and the angular rotation on each axis for each volume. All participants' BOLD data were within the defined motion thresholds (i.e., translational or rotational motion parameters <2 mm or 2°). We also calculated frame-wise displacement (FD), which indexes the volume-to-volume changes in head position. Several nuisance covariates (the linear drift, the estimated motion parameters based on the Friston-24 model, the spike volumes with FD > 0.5 mm, the white matter signal, and the cerebrospinal fluid signal) were regressed out from the data. The datasets were then band-pass filtered using a frequency range of 0.01 to 0.1 Hz. In the normalization step, individual structural images were firstly co-registered with the mean functional image; then the transformed structural images were segmented and normalized to the Montreal Neurological Institute (MNI) space using a high-level nonlinear warping algorithm, that is, the diffeomorphic anatomical registration through the exponentiated Lie algebra (DARTEL) technique (Ashburner, 2007). Finally, each filtered functional volume was spatially normalized to the MNI space using the deformation parameters estimated during the above step and resampled into a 3-mm cubic voxel.

2.5. Functional stability calculation

Based on a previous published study (Li et al., 2020), the calculation process of functional stability is summarized in Fig. 1. Firstly, dynamic functional connectivity analysis was performed using a sliding-window approach (Hutchison et al., 2013), with the window size being 96 s (40 TR) and the sliding step being 4.8 s (2 TR). For a given voxel j, we computed Pearson's correlation coefficients between its time series and those of all other voxels within the gray matter mask. This process yielded a sequence of dynamic functional connectivity maps for voxel j across different time windows. Subsequently, the functional stability of voxel j was assessed using Kendall's concordance coefficient (KCC) applied to the dynamic functional connectivity maps across various time windows, employing the following equation:

$$\mathrm{KCC} = \frac{\sum_{n=1}^{N} R_n^2 - \frac{1}{N}\left(\sum_{n=1}^{N} R_n\right)^2}{\frac{1}{12}K^2\left(N^3 - N\right)}$$

In this equation, K represents the number of time windows, N signifies the total number of connections between voxel j and all other voxels within the gray matter mask, and R_n stands for the sum of rank for the n-th connection across all windows. To be specific, all subjects had the same number of time windows, ensuring an equivalent K value for each participant. The gray matter mask employed for restricting analyses in this investigation was generated by applying a threshold of 0.2 to the mean gray matter density map from all participants and subsequently intersected with a group-level mask encompassing 90 % coverage of all functional images. Therefore, N was equivalent to the total number of voxels within the mask minus one, a value consistent across all participants. For the n-th connection ($n = 1, 2, \cdots, N$), R_n was designated as the sum of rank across all K windows, i.e., $R_n = R_n(1) + R_n(2) + \ldots + R_n(K)$. For each time window, connections were ranked according to their functional connectivity strength. To ensure that results were not biased by distinct numbers of connections, we did not apply any thresholding and a fully connected matrix consisting of both positive and negative connections was used for ranking, with the sign of negative connections rather than their absolute values considered in the ranking. Once the functional stability maps were generated, they underwent an additional standardization process into z-scores. This entailed subtracting the mean and dividing by the standard deviation of the global values within the gray matter mask so that they could be averaged and compared across subjects. Ultimately, these stability maps underwent spatial smoothing utilizing a Gaussian kernel with a full-width at half maximum (FWHM) of 6 mm × 6 mm × 6 mm. For a voxel or region, an elevated stability value (KCC) indicates a greater degree of coherence and steadiness in its dynamic functional architecture over time. Conversely, a diminished stability value signifies its

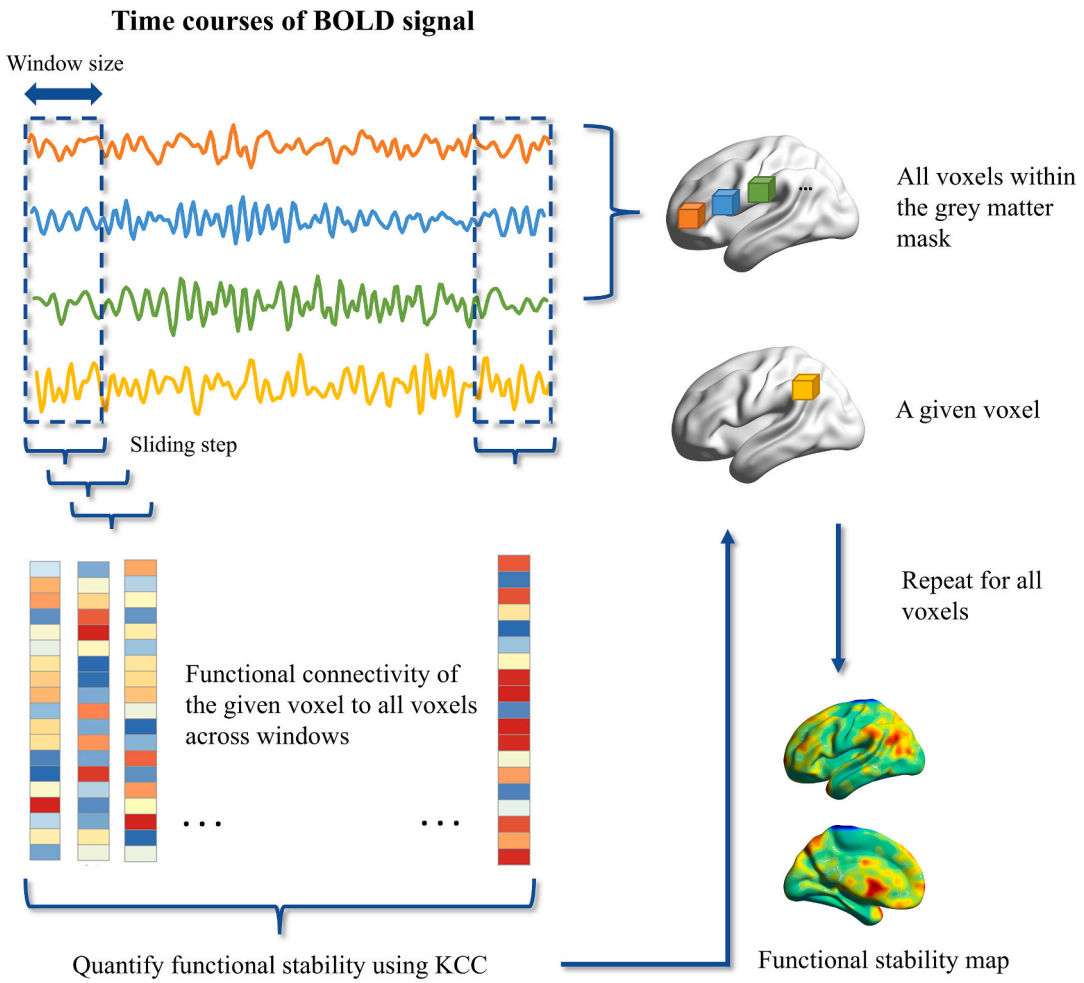

Fig. 1. A schematic diagram illustrating the process for calculating functional stability. First, dynamic functional connectivity was calculated using a sliding-window method. For a given voxel, a series of dynamic functional connectivity maps were generated by computing Pearson's correlation coefficients between its time series and those of all other voxels within the gray matter mask across different time windows. Next, the functional stability of that voxel was measured using the KCC applied to these dynamic functional connectivity maps with time windows as raters. Ultimately, a functional stability map was created by performing the same calculation described above for every voxel within the gray matter mask. Abbreviations: BOLD, blood oxygen level-dependent; KCC, Kendall's concordance coefficient.

capacity to frequently and swiftly transition between distinct brain states.

2.6. Statistical analysis

All calculations, statistical analyses, and visualizations were conducted using MATLAB (version 2019b, The MathWorks Inc., Natick, MA, USA) and Python (version 3.8). The MDD and HC groups were compared using two-sample *t*-tests for normally distributed values, Mann-Whitney *U* tests for non-normally distributed values regarding age and clinical characteristics, and a chi-squared test for gender distribution.

To examine the impact of ECT treatment on clinical symptoms in MDD patients, a linear mixed effects (LME) model (Bernal-Rusiel et al., 2013) was utilized to evaluate the changes in HRSD scores between MDD patients and HCs across two time points. The model included group (MDD vs. HCs) and time (baseline vs. follow-up) as fixed factors, with individual participants as a random factor. Post-hoc analysis involved two-sample *t*-tests to compare groups and paired *t*-tests to evaluate changes following ECT. Multiple comparison correction was performed using the Bonferroni method. The LME model and two-sample *t*-tests were conducted with age and sex as covariates, setting the significance threshold at $p < 0.05$.

2.7. Functional stability analysis

To explore the impact of ECT on brain functional stability in MDD patients, an LME model was employed to investigate the interaction effect of group and time on brain functional stability maps. In this model, group (MDD vs. HCs) and time (baseline vs. follow-up) were set as fixed factors, and the participant was set as the random factor. For these voxel-based analyses, we conducted multiple comparison correction using the cluster-level false discovery rate (FDR) method, resulting in a cluster-defining threshold of $p = 0.001$ and a corrected cluster significance of $p < 0.05$. Brain regions with significant interaction effects were defined as regions of interest (ROIs), from which functional stability values were extracted for post-hoc comparisons. Post-hoc analyses were conducted using two-sample *t*-tests to compare groups and paired *t*-tests to evaluate differences at two scans. The LME model and two-sample *t*-tests included age, sex, and mean FD as covariates, and the paired *t*-tests were conducted with mean FD as a covariate.

The relationship between ECT-induced changes in functional stability and clinical symptoms in MDD patients was assessed using Pearson's correlation analysis. Specifically, we examined the associations between the rates of change in functional stability (defined as post-ECT values minus pre-ECT values, divided by the absolute value of the pre-ECT values) in ROIs with significant interaction effects and the

treatment-related rate of change in HRSD scores. The significance threshold was determined at $p < 0.05$ and adjusted for multiple testing using the FDR method.

2.8. Comparison between remitters and non-remitters

One of the unresolved issues regarding ECT is its variability in efficacy. While ECT is generally effective for MDD patients, it fails to achieve the expected outcomes in certain patient groups. To investigate the factors that might contribute to this variability in efficacy, we classified the MDD patients into two groups based on whether they achieved remission after ECT: 39 in the remitters group and 19 in the non-remitters group. Patients with a post-ECT HRSD score of <7 were classified as remitters (Bech et al., 2005; Möller, 2008). The basic information of the two subgroups is shown in Table 2.

The statistical methods used for analyzing demographic and clinical data were consistent with those employed in the MDD vs. HC analysis. An LME model and subsequent post-hoc tests were employed to compare remitter and non-remitter groups to analyze functional stability. Pearson's correlations were performed to investigate whether changes in functional stability were associated with changes in clinical symptoms after ECT. These correlations examined the relationship between the rate of change in functional stability in ROIs showing significant interaction effects in subgroup analysis and the rate of change in HRSD scores. All analyses were adjusted for age, sex, and mean FD, with a significance threshold set at $p < 0.05$, applying FDR correction.

Table 2
Demographic and clinical measurements of remitters and non-remitters.

Characteristic	Remitters (n = 39)	Non-remitters (n = 19)	Statistics	p-Value
Age (years)	41.38 ± 11.35	35.74 ± 12.59	$t = 1.716$[a]	0.092
Gender (male/female)	11/28	4/15	$\chi^2 = 0.341$[b]	0.559
Scan interval (days)	19(18,22)	20(18,24)	$U = 197.00$[c]	0.443
ECT sessions (n)	8(8,8)	8(8,10)	$U = 197.00$[c]	0.154
Illness duration (months)	48(10,132)	24(5.5,42)	$U = 450.000$[c]	0.187
Episodes (first/recurrence, n)	11/28	9/10	$\chi^2 = 2.07$[b]	0.150
HRSD scores			$F = 7.291$[d]	0.009
Baseline	21.59 ± 6.15	26.53 ± 5.19	$t = -3.012$[a]	0.004
After ECT	3.54 ± 2.37	13.53 ± 3.96	$t = -10.136$[a]	<0.001
Medicine category			NA	NA
SSRIs	28	13	NA	NA
SNRIs	10	6	NA	NA
SARIs	2	1	NA	NA
NaSSAs	9	5	NA	NA
APs	20	10	NA	NA
ACs[e]	6	5	NA	NA
NBH	14	5	NA	NA

Note: Values are shown as the mean value ± standard deviation median (Q1, Q3). Abbreviations: ECT, electroconvulsive therapy; HRSD, Hamilton rating scale of depression; SSRIs, selective serotonin reuptake inhibitors; SNRIs, serotonin-norepinephrine reuptake inhibitors; SARIs, serotonin antagonist/reuptake inhibitors; NaSSAs, norepinephrine and specificity serotonergic antidepressants; APs, antipsychotics; ACs, Anticonvulsants; NBH: Non-benzodiazepine hypnotic; NA, not applicable.

[a] Two-sample t-tests.

[b] Pearson chi-squared test.

[c] Mann-Whitney U tests.

[d] Linear mixed effects model.

[e] ACs primarily consist of valproate and benzodiazepines, used for mood stabilization and managing insomnia.

2.9. Validation analysis

The following procedures were taken to further validate our findings. To determine whether our primary findings were influenced by the selection of different sliding window parameters, we computed functional stability using three additional combinations of window size and sliding step (window size = 30 TR and sliding step = 2 TR; window size = 50 TR and sliding step = 2 TR; window size = 40 TR and sliding step = 1 TR) and then repeated the above analyses. Second, considering the potential impact of spatial smoothing on the outcomes, we applied Gaussian kernels of 8 mm FWHM to smooth functional stability maps and subsequently repeated the voxel-wise group comparison analyses.

3. Results

3.1. Demographic and clinical characteristics

The demographic and clinical data of MDD patients and HCs are shown in Table 1. There were no significant differences in age or gender between the MDD and HC groups (all $p > 0.05$). We noted a significant group-by-time interaction effect ($F = 245.05$, $p < 0.001$, $\text{Eta}^2 = 0.719$), as well as a main effect of group ($F = 308.80$, $p < 0.001$, $\text{Eta}^2 = 0.763$) on the HRSD scores. However, the main effect of time was not significant ($F = 0.35$, $p = 0.556$, $\text{Eta}^2 = 0.004$). Post-hoc analyses revealed that HRSD scores decreased in MDD patients following ECT treatment ($t = -19.35$, $p < 0.001$, Cohen's $d = -2.54$, mean ECT session: 8.33), whereas no significant changes were observed in HRSD scores between scans for the HC group ($t = -1.891$, $p = 0.268$, Cohen's $d = -0.21$).Meanwhile, the HRSD scores of the MDD group were significantly higher than those of the HC group before and after ECT (all $p < 0.001$) (Fig. 2b and Table 1).

3.2. Effects of ECT on functional stability in MDD patients

Analysis of functional stability revealed a significant group-by-time interaction effect in multiple brain regions (all $p < 0.05$, FDR corrected, Fig. 2c and Table 3), including bilateral middle frontal gyrus, orbital part (ORBmid), bilateral angular gyrus (ANG), and right fusiform gyrus (FFG). Post-hoc analysis revealed significant increases in the functional stability of the bilateral ORBmid and bilateral ANG after ECT in MDD patients; meanwhile, we observed a reduction in functional stability in the right FFG of MDD patients after ECT (all $p < 0.05$, FDR corrected). However, no significant changes were observed in functional stability between scans for the HC group. Among them, in bilateral ORBmid and bilateral ANG, the functional stability values of the MDD group after ECT were significantly higher than those of the HC group (all $p < 0.001$), but in FFG, the functional stability values of the MDD group were significantly lower than those of the HC group ($p < 0.001$). Among them, we showed the post-hoc results of two typical regions as violin plots (Fig. 2d). The full results of the post-hoc test are available in Fig. S1.

3.3. Correlations between the rate of change in functional stability and clinical variables

We examined the correlation between the rate of change in the HRSD scores and the rate of change in functional stability of ROIs with significant interaction effects. However, after multiple comparison corrections, no significant correlation was observed in MDD patients (all $p > 0.05$, FDR corrected).

3.4. ECT-induced differences in functional stability in remitters vs. non-remitters

Comparison between the remitter and non-remitter subgroups revealed no significant differences in age, gender, scan intervals, number of ECT sessions, duration of illness, or number of episodes (all $p >$

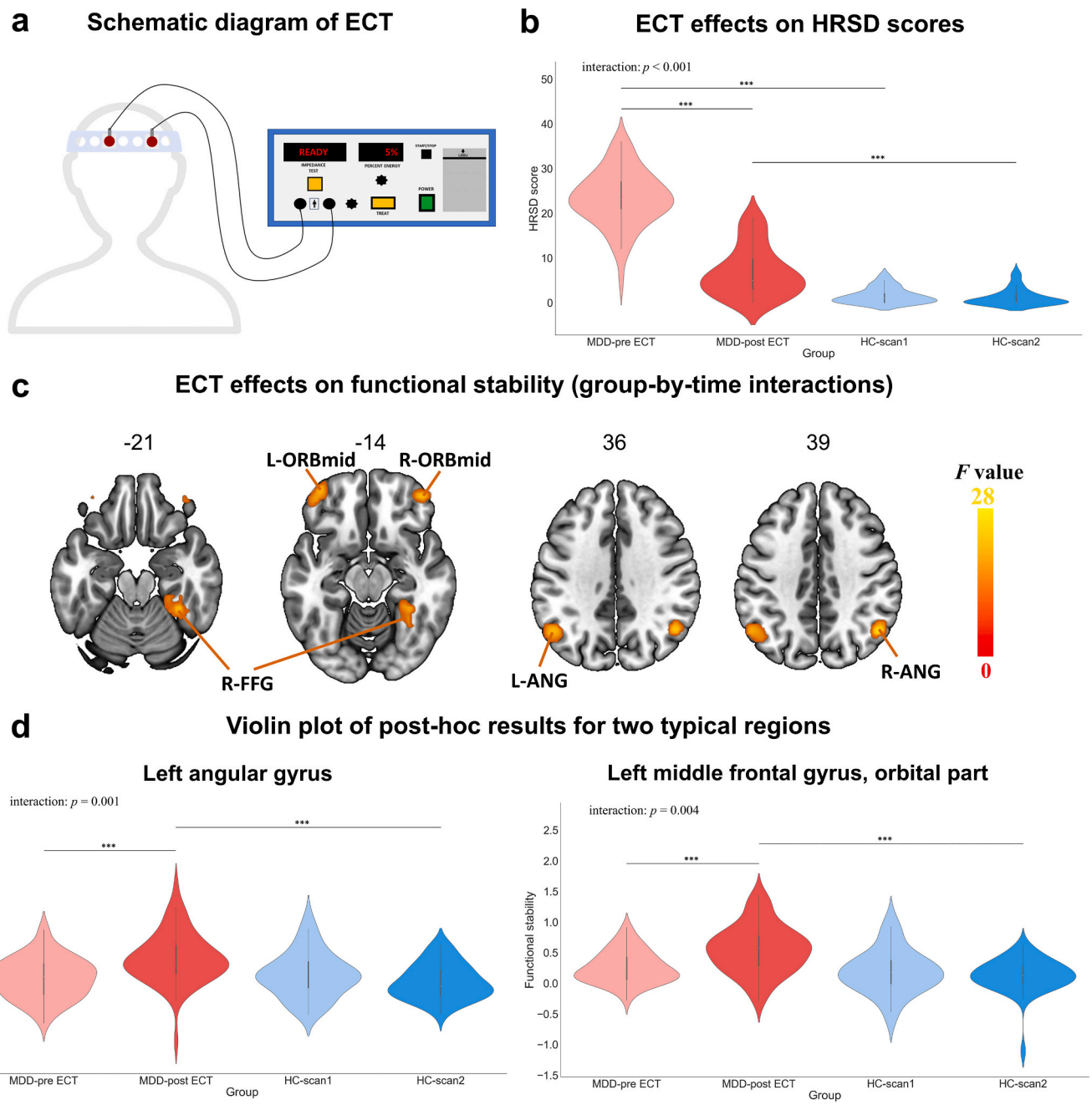

Fig. 2. ECT paradigm and its effects on clinical symptom and functional stability in MDD patients. a. Schematic diagram of bifrontal ECT treatment plan. b. Comparison of HRSD score between MDD and HC group at two scans. (***, $p < 0.001$). c. Brain regions with significant interaction effects in functional stability between MDD and HC group based on ECT ($p < 0.05$, FDR corrected). d. Violin plot of post-hoc results for two typical regions. (***, $p < 0.001$). Abbreviations: ECT, electroconvulsive therapy; HRSD, Hamilton Rating Scale for Depression; MDD, major depressive disorder patients; HC, healthy control; FFG, fusiform gyrus; ORBmid, middle frontal gyrus, orbital part; ANG, angular gyrus; L, left; R, right.

Table 3
Brain regions showing significant group-by-time interaction effects in functional stability between MDD and HCs.

Clusters	Brain regions	Abbreviation	Cluster size (voxels)	Peak MNI coordinates (mm)			Peak *F* values
				x	y	z	
Cluster 1	Middle frontal gyrus, orbital part (L)	L-ORBmid	99	−39	54	−12	28.96
Cluster 2	Middle frontal gyrus, orbital part (R)	R-ORBmid	56	42	48	−18	27.20
Cluster 3	Angular gyrus (L)	L-ANG	162	−51	−60	36	21.62
Cluster 4	Angular gyrus (R)	R-ANG	72	51	−60	39	28.70
Cluster 5	Fusiform gyrus (R)	R-FFG	110	33	−42	−21	22.04

Abbreviations: MDD, major depressive disorder; HC, healthy control; MNI, Montreal Neurological Institute; L, left; R, right.

0.05, Table 2). Analysis of HRSD scores identified a significant group-by-time interaction effect ($F = 7.29$, $p = 0.009$, $Eta^2 = 0.119$), as well as a main effect of group ($F = 58.34$, $p = 0.009$, $Eta^2 = 0.519$). However, the main effect of time was not significant ($F = 1.80$, $p = 0.185$, $Eta^2 = 0.032$). Post-hoc analysis indicated that after ECT, the HRSD scores in both remitters and non-remitters significantly decreased (remitters: $t = -18.76$, $p < 0.001$, Cohen's $d = -3.00$; non-remitters: $t = -9.09$, $p < 0.001$, Cohen's $d = -2.08$). However, the post-treatment HRSD scores of the non-remitters remained significantly higher than those of the remitters ($t = 11.99$, $p < 0.001$, Cohen's $d = 3.35$) (Fig. 3a).

Analysis of functional stability revealed a significant group-by-time interaction effect in the right hippocampus ($F = 27.38$, $p = 0.02$, FDR corrected) (Table 4). Post-hoc analysis showed that at baseline, there was no significant difference in the functional stability values of the right hippocampus between remitters and non-remitters ($t = 1.398$, $p = 0.168$, Cohen's $d = 0.35$). After ECT, the functional stability values of the right hippocampus in remitters significantly decreased ($t = -4.988$, $p < 0.001$, Cohen's $d = -0.80$), while in non-remitters, these values

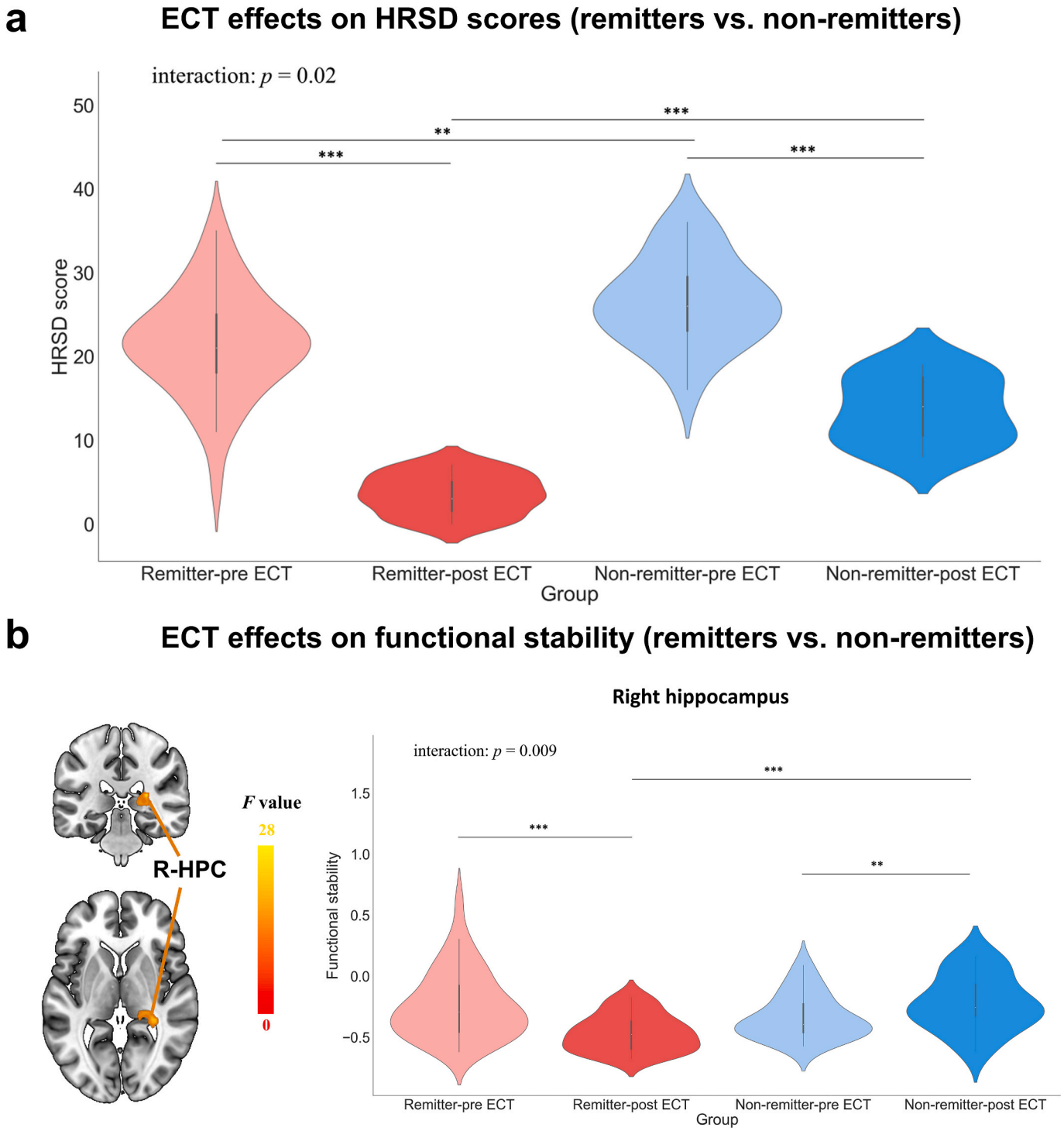

Fig. 3. ECT effects on HRSD scores and functional stability in remitters and non-remitters. a. Comparison of HRSD scores between remitters and non-remitters group based on ECT (**, $p < 0.01$; ***, $p < 0.001$). b. Comparison of functional stability and post-hoc analysis between remitters and non-remitters group based on ECT (**, $p < 0.01$; ***, $p < 0.001$). Abbreviations: ECT, electroconvulsive therapy; HRSD, Hamilton Rating Scale for Depression; HPC, hippocampus; R, right.

Table 4
Brain regions showing significant group-by-time interaction effects in functional stability between remitters and non-remitters.

Clusters	Brain regions	Abbreviation	Cluster size (voxels)	Peak MNI Coordinates (mm)			Peak *F* values
				x	y	z	
Cluster 1	Hippocampus (R)	R-HPC	77	27	−30	12	27.38

Abbreviations: MNI, Montreal Neurological Institute; R, right.

significantly increased ($t = 3.185$, $p = 0.005$, Cohen's $d = 0.73$), resulting in significantly higher functional stability values in non-remitters compared to remitters after treatment ($t = 4.962$, $p < 0.001$, Cohen's $d = 1.38$).

Subsequently, we extracted the functional stability values of the right hippocampus and calculated the change rates for both remitters and non-remitters. We then performed a correlation analysis between these stability change rates and the change rates of the HRSD scores, but no significant correlations were found (all $p > 0.05$, FDR corrected).

3.5. Validation analysis

First, our primary results held when employing functional stability calculated from three other combinations of window size and sliding step, implying that variations in sliding window parameters had minimal impact on our functional stability analyses (Figs. S2 and S3). Moreover, when applying Gaussian kernels with full width at half maximum (FWHM) values of 8 mm to smooth functional stability maps, we observed that the voxel-wise group comparison outcomes were similar to those obtained using a 6 mm FWHM Gaussian kernel.

4. Discussion

In this study, we utilized functional stability, a state-of-the-art analytical method, to explore the impact of ECT on brain dynamic function in MDD. The results showed that after ECT, there was a significant increase in functional stability in the bilateral ORBmid and bilateral ANG, whereas there was a significant decrease in functional stability in the right fusiform gyrus. Additionally, we conducted a subgroup analysis by dividing MDD patients into remitters and non-remitters based on their post-ECT HRSD scores. The subgroup analysis revealed a significant group-by-time interaction effect on functional stability in the right hippocampus, with remitters showing a significant decrease after ECT, while non-remitters exhibited a significant increase. These findings elucidate the mechanisms by which ECT modulates brain function and depressive symptoms, suggesting that functional stability could serve as a potential biological marker for ECT treatment in MDD.

In our previous work using resting-state fMRI, we identified abnormal local brain indices, such as changes in brain entropy following ECT (Fan et al., 2024) and increased nodal degree in specific regions, which negatively correlated with post-ECT improvements in depressive symptoms(Wu et al., 2022). These findings highlight the modulatory effect of ECT on the mean activity levels of local brain regions. Furthermore, at the large-scale functional network level, we observed alterations in graph-theoretical metrics, including increased shortest path length, decreased global efficiency (Li et al., 2022), and changes in the default mode network (Li et al., 2023). Although these studies illuminate how ECT may modulate local brain regions and networks from a static, averaged activity perspective, they do not address the potential neural mechanisms from a dynamic activity standpoint.

Functional stability is a voxel-wise measurement derived from dynamic functional connectivity analysis (Li et al., 2020). A higher stability value for a voxel indicates a more consistent and stable dynamic functional architecture over time. In contrast, a lower stability value signifies the voxel's capacity to frequently and rapidly transition between different brain states. Increased functional stability in bilateral ANG and bilateral ORBmid were found in MDD patients after ECT. ANG has been suggested to be one of the central areas of the default mode network (DMN) involved in introspective processing, emotional processing, memory, and spontaneous cognition (Andrews-Hanna et al., 2010; Raichle et al., 2001). Numerous studies have shown that structural and functional changes of ANG are involved in the pathogenesis of depression. For example, a whole-brain functional connectivity study has shown that depressed patients have reduced functional connectivity strength (FCS) in the left ANG (Lai et al., 2017). The coherence-based regional homogeneity of right ANG in patients with late-life depression was significantly lower than that in normal subjects (Liu et al., 2012). Lee et al. found that reduced gray matter volume in the left ANG in depressed patients was associated with suicide attempts (Lee et al., 2016). ANG has been used as an observation index for the treatment effect and prognosis evaluation of depression since it is related to the occurrence of various depressed symptoms. A significant increase in gray matter volume was observed in the right ANG after TMS treatment in patients with depression (Lan et al., 2016). The FCS of the left ANG increased significantly after ECT in depressed patients (Wei et al., 2018). The present study found that ECT can up-regulate the functional stability of ANG, which is consistent with the results of the above-mentioned research.

The orbitofrontal cortex (OFC) is a key brain region in reward value, mood and emotion (Rolls et al., 2020). Abnormal function or structure of the OFC disrupts the reward circuit in depressed patients, consequently resulting in anhedonia symptoms (O'Doherty et al., 2001; Rolls, 2017). Studies in adult depression have documented that reduced superior frontal gyrus activity in response to loss is associated with increased depressive rumination symptoms (Schiller et al., 2013). In a resting-state fMRI investigation, effective connectivity directed to the medial OFC from areas including the parahippocampal gyrus, temporal pole, inferior temporal gyrus and amygdala was found decreased in depression (Rolls et al., 2018). ORBmid, as one of the components of OFC, has also been confirmed to be involved in the pathogenesis of depression. For example, the functional connectivity between the insula and the left ORBmid in depressed patients is proven reduced (Guo et al., 2015). Additionally, the ALFF value of the right ORBmid is lower in depressed patients with anxiety compared to health controls (Zhao et al., 2019). Our research demonstrated that ECT can enhance the functional stability of the ORBmid to improve depressive symptoms, which corroborates the aforementioned conclusions.

Additionally, this study found that the functional stability of the right fusiform gyrus in MDD patients significantly decreased after ECT. The fusiform gyrus, a critical part of the visual cortex, plays a significant role in the perception and processing of emotions when faces are presented as stimuli (Haxby et al., 2000; Zhang et al., 2016).

The fusiform gyrus is closely associated with MDD. Studies have shown that both the structure and function of the fusiform gyrus are abnormal in MDD patients. Specifically, research has found that MDD patients exhibit significantly reduced cortical folding in the right fusiform gyrus, along with decreased functional connectivity between this region and sensorimotor areas (such as the precentral and postcentral gyri) as well as the right superior temporal gyrus (Chen et al., 2021). In a task-based fMRI study measuring neural responses to happy and sad facial expressions in healthy individuals and MDD patients, it was found that healthy individuals exhibited linear increases in bilateral fusiform gyrus responses to increasingly happy expressions. In contrast, MDD patients showed linear increases in right fusiform gyrus responses to

increasingly sad expressions. Additionally, among MDD patients, there was a negative correlation between depression severity and the neural response strength in the right fusiform gyrus to happy expressions (Surguladze et al., 2005). These findings highlight the critical role of the fusiform gyrus in emotional processing and the pathophysiology of depression. Based on the findings of this study, we speculate that the functional stability of the right fusiform gyrus may be modulated by ECT, leading to a decrease in stability. This allows for more rapid and flexible functional transitions, enhancing the accuracy and flexibility of facial expression recognition. Such changes may help regulate implicit and explicit attentional bias patterns, improving depressive symptoms.

Although ECT is an effective neuromodulation method for treating MDD, its efficacy varies significantly among different patients, and the reasons for this variability remain unclear (Haq et al., 2015; Nygren et al., 2023). To investigate the differences in treatment outcomes, we categorized MDD patients into remitters and non-remitters based on whether their HRSD score was below 7 after ECT. The functional stability analysis revealed that although there was no significant difference in functional stability of in the right hippocampus between remitters and non-remitters, the functional stability significantly decreased in remitters but increased dramatically in non-remitters after ECT, presenting opposite results between the two groups. The hippocampus not only plays an important role in memory and learning but also in emotion regulation and emotion-related disorders. The hippocampus, together with the amygdala and prefrontal cortex, participates in the processing and regulation of emotions(Davidson and Irwin, 1999). The amygdala is responsible for generating emotional responses, while the hippocampus helps link emotions with memories (Phelps, 2004). For instance, the hippocampus is crucial in the encoding and retrieval of emotional events in memory (Kensinger and Schacter, 2005).

Negative cognitive bias is a crucial cognitive psychological mechanism in the onset of depression. Among these biases, negative emotional memory bias is a core element. MDD patients tend to have stronger memories for negative emotions compared to positive emotions (Disner et al., 2011). Prolonged immersion in negative emotions can lead to symptoms such as emotional downturns, anhedonia, and even suicidal tendencies (Harmer and Cowen, 2011; Roiser et al., 2012). Previous research has found that there are neuronal groups within the hippocampal region dedicated to processing both positive and negative emotional memories. These groups use distinct neural projection patterns to optimize the integration of different types of memory information (Shpokayte et al., 2022). Animal experiments have discovered that optogenetic activation of hippocampal cells associated with positive memories can alleviate depressive-like behaviors in mice. This method not only shows immediate effects but also promotes neurogenesis over the long term, offering a potential new approach for treating depression (Ramirez et al., 2015). Additionally, previous study has shown that changes in hippocampal function are associated with improvements in depressive symptoms after ECT (Bai et al., 2019). Therefore, combining the findings of this study, we speculate that in the remitters group, the decreased functional stability of the right hippocampus following ECT enables faster and more flexible emotional encoding, retrieval, and switching, thus improving emotional memory bias. In contrast, in the non-remitters group, increased functional stability post-ECT is detrimental to emotional switching and the improvement of emotional memory bias, leading to less significant alleviation of depressive symptoms. This suggests that focusing on hippocampal functional changes could be crucial for assessing the antidepressant effects of ECT.

Neurocognitive impairment is a common side effect of ECT, making the reduction of such adverse effects a significant research focus. Non-convulsive electrotherapy (NET) is an emerging treatment for MDD that involves electrical stimulation of the brain in a manner similar to standard ECT procedures. Previous studies have shown that NET, when used as an adjunctive therapy, may be a safe, well-tolerated, and effective treatment for depression without causing severe neurocognitive deficits (Cai et al., 2021; Zhang et al., 2024). Additionally, transnasal humidified rapid-insufflation ventilatory exchange (THRIVE) is a novel and effective ventilation method that has been incorporated into ECT to enhance patient tolerability and reduce the risk of complications. As a high-flow nasal oxygen ventilation technique, THRIVE improves oxygenation and ventilation management, helping to maintain more stable physiological parameters and potentially minimizing cognitive impairment caused by hypoxia or hemodynamic fluctuations during ECT (Deng et al., 2024). Preliminary research indicates that ECT performed with THRIVE may be associated with fewer cognitive side effects, although further clinical studies are necessary to validate these findings.

5. Limitations

The current findings must be interpreted in light of the following limitations. First, due to the limited sample size, our research lacks replication and requires reanalysis of independent data. A larger sample is needed in future studies to replicate the current experiment and reduce the impact of experimental errors. Second, we cannot rule out the effect of medication on our results. The patients included in the treatment were receiving medication, which can improve depressive symptoms and potentially alter brain function. Future studies should include patients with depression who are not yet on medication, and perform stratification analysis or calculate medication weights as covariates. Additionally, future research should consider adding a control group of MDD patients who are only receiving medication to further assess the unique effects of ECT.

6. Conclusion

In summary, our data demonstrated the modulatory effect of ECT on brain functional stability in MDD patients and further revealed the differences in this modulation between patients with and without clinical remission. This study may advance our understanding of the neural effects of ECT in MDD from the perspective of dynamic functional stability, highlighting that functional stability can serve as a potential prognostic biomarker that can be used to monitor the efficacy of ECT treatment or to stratify MDD patients to optimize disease management and treatment strategies.

CRediT authorship contribution statement

Dongpeng Wu: Writing – review & editing, Writing – original draft, Methodology, Data curation. **Yue Yu:** Software, Methodology, Data curation. **Hongping Wang:** Validation, Software, Resources, Data curation. **Jiahua Zhang:** Validation, Software, Methodology. **Jingyi You:** Software, Resources, Methodology. **Yiao Kai:** Visualization, Validation, Software. **Yue Zhao:** Visualization, Validation, Supervision. **Yue Wu:** Validation, Software. **Kai Wang:** Writing – review & editing, Supervision. **Yanghua Tian:** Writing – review & editing, Project administration, Funding acquisition, Conceptualization.

Funding

This work was supported by National Natural Science Foundation of China (Grant Nos. U24A20702 and 32071054) and Research Fund of Anhui Institute of Translational Medicine (Grant No. 2021zhyx-B10).

Declaration of competing interest

The authors state that there are no known financial conflicts of interest or personal relationships that might seem to affect the work presented in this paper.

Acknowledgments

We thank Anhui Mental Health Center for providing case resources

and the University of Science and Technology of China for the MRI scanning facilities.

Appendix A. Supplementary data

Supplementary data to this article can be found online at https://doi.org/10.1016/j.jad.2025.01.066.

References

Andrews-Hanna, J.R., Reidler, J.S., Huang, C., Buckner, R.L., 2010. Evidence for the default network's role in spontaneous cognition. J. Neurophysiol. 104, 322–335. https://doi.org/10.1152/jn.00830.2009.

Ashburner, J., 2007. A fast diffeomorphic image registration algorithm. NeuroImage 38, 95–113. https://doi.org/10.1016/j.neuroimage.2007.07.007.

Bai, T., Wei, Q., Xie, W., Wang, A., Wang, J., Ji, G.J., et al., 2019. Hippocampal-subregion functional alterations associated with antidepressant effects and cognitive impairments of electroconvulsive therapy. Psychol. Med. 49, 1357–1364. https://doi.org/10.1017/s0033291718002684.

Barkhof, F., Haller, S., Rombouts, S.A., 2014. Resting-state functional MR imaging: a new window to the brain. Radiology 272, 29–49. https://doi.org/10.1148/radiol.14132388.

Bech, P., Engelhardt, N., Evans, K.R., Gibertini, M., Kalali, A.H., Kobak, K.A., et al., 2005. Why the Hamilton Depression Rating Scale endures. Am. J. Psychiatry 162, 2396 author reply 7-8. https://doi.org/10.1176/appi.ajp.162.12.2396.

Bernal-Rusiel, J.L., Greve, D.N., Reuter, M., Fischl, B., Sabuncu, M.R., 2013. Statistical analysis of longitudinal neuroimage data with Linear Mixed Effects models. NeuroImage 66, 249–260. https://doi.org/10.1016/j.neuroimage.2012.10.065.

Biswal, B., Yetkin, F.Z., Haughton, V.M., Hyde, J.S., 1995. Functional connectivity in the motor cortex of resting human brain using echo-planar MRI. Magn. Reson. Med. 34, 537–541. https://doi.org/10.1002/mrm.1910340409.

Cai, D.B., Zhou, H.R., Liang, W.N., Gu, L.M., He, M., Huang, X., et al., 2021. Adjunctive nonconvulsive electrotherapy for patients with depression: a systematic review. Psychiatry Q. 92, 1645–1656. https://doi.org/10.1007/s11126-021-09936-5.

Chang, C., Glover, G.H., 2010. Time-frequency dynamics of resting-state brain connectivity measured with fMRI. NeuroImage 50, 81–98. https://doi.org/10.1016/j.neuroimage.2009.12.011.

Chen, C., Liu, Z., Zuo, J., Xi, C., Long, Y., Li, M.D., et al., 2021. Decreased cortical folding of the fusiform gyrus and its hypoconnectivity with sensorimotor areas in major depressive disorder. J. Affect. Disord. 295, 657–664. https://doi.org/10.1016/j.jad.2021.08.148.

Chen, G., Chen, P., Gong, J., Jia, Y., Zhong, S., Chen, F., et al., 2022. Shared and specific patterns of dynamic functional connectivity variability of striato-cortical circuitry in unmedicated bipolar and major depressive disorders. Psychol. Med. 52, 747–756. https://doi.org/10.1017/s0033291720002378.

Davidson, R.J., Irwin, W., 1999. The functional neuroanatomy of emotion and affective style. Trends Cogn. Sci. 3, 11–21. https://doi.org/10.1016/s1364-6613(98)01265-0.

Dehaene, S., Lau, H., Kouider, S., 2017. What is consciousness, and could machines have it? Science (New York, N.Y.) 358, 486–492. https://doi.org/10.1126/science.aan8871.

Demirtaş, M., Tornador, C., Falcón, C., López-Solà, M., Hernández-Ribas, R., Pujol, J., et al., 2016. Dynamic functional connectivity reveals altered variability in functional connectivity among patients with major depressive disorder. Hum. Brain Mapp. 37, 2918–2930. https://doi.org/10.1002/hbm.23215.

Deng, C.J., Nie, S., Mai, J.X., Zou, D.C., Deng, W., Huang, X., et al., 2024. Narrative review and consensus recommendations for the use of transnasal humidified rapid-insufflation ventilatory exchange in modified electroconvulsive therapy. Alpha Psychiatry. 25, 282–289. https://doi.org/10.5152/alphapsychiatry.2024.231463.

Disner, S.G., Beevers, C.G., Haigh, E.A., Beck, A.T., 2011. Neural mechanisms of the cognitive model of depression. Nat. Rev. Neurosci. 12, 467–477. https://doi.org/10.1038/nrn3027.

Fan, S., Zhang, J., Wu, Y., Yu, Y., Zheng, H., Guo, Y.Y., et al., 2024. Changed brain entropy and functional connectivity patterns induced by electroconvulsive therapy in majoy depression disorder. Psychiatry Res. Neuroimaging 339, 111788. https://doi.org/10.1016/j.pscychresns.2024.111788.

Filippi, M., Spinelli, E.G., Cividini, C., Agosta, F., 2019. Resting state dynamic functional connectivity in neurodegenerative conditions: a review of magnetic resonance imaging findings. Front. Neurosci. 13, 657. https://doi.org/10.3389/fnins.2019.00657.

Fox, M.D., Greicius, M., 2010. Clinical applications of resting state functional connectivity. Front. Syst. Neurosci. 4, 19. https://doi.org/10.3389/fnsys.2010.00019.

Fu, Z., Abbott, C.C., Miller, J., Deng, Z.D., McClintock, S.M., Sendi, M.S.E., et al., 2023. Cerebro-cerebellar functional neuroplasticity mediates the effect of electric field on electroconvulsive therapy outcomes. Transl. Psychiatry 13, 43. https://doi.org/10.1038/s41398-023-02312-w.

Guo, W., Liu, F., Xiao, C., Zhang, Z., Liu, J., Yu, M., et al., 2015. Decreased insular connectivity in drug-naive major depressive disorder at rest. J. Affect. Disord. 179, 31–37. https://doi.org/10.1016/j.jad.2015.03.028.

Hamilton, M., 1967. Development of a rating scale for primary depressive illness. Br. J. Soc. Clin. Psychol. 6, 278–296. https://doi.org/10.1111/j.2044-8260.1967.tb00530.x.

Haq, A.U., Sitzmann, A.F., Goldman, M.L., Maixner, D.F., Mickey, B.J., 2015. Response of depression to electroconvulsive therapy: a meta-analysis of clinical predictors. J. Clin. Psychiatry 76, 1374–1384. https://doi.org/10.4088/JCP.14r09528.

Harmer, C.J., Cowen, P.J., 2011. Goodwin GMJJop. Efficacy markers in depression. 25, 1148–1158.

Haxby, J.V., Hoffman, E.A., Gobbini, M.I., 2000. The distributed human neural system for face perception. Trends Cogn. Sci. 4, 223–233. https://doi.org/10.1016/s1364-6613(00)01482-0.

Hutchison, R.M., Womelsdorf, T., Allen, E.A., Bandettini, P.A., Calhoun, V.D., Corbetta, M., et al., 2013. Dynamic functional connectivity: promise, issues, and interpretations. NeuroImage 80, 360–378. https://doi.org/10.1016/j.neuroimage.2013.05.079.

Kaiser, R.H., Andrews-Hanna, J.R., Wager, T.D., Pizzagalli, D.A., 2015. Large-scale network dysfunction in major depressive disorder: a meta-analysis of resting-state functional connectivity. JAMA Psychiatry 72, 603–611. https://doi.org/10.1001/jamapsychiatry.2015.0071.

Kensinger, E.A., Schacter, D.L., 2005. Retrieving accurate and distorted memories: neuroimaging evidence for effects of emotion. NeuroImage 27, 167–177. https://doi.org/10.1016/j.neuroimage.2005.03.038.

Lai, C.H., Wu, Y.T., Hou, Y.M., 2017. Functional network-based statistics in depression: theory of mind subnetwork and importance of parietal region. J. Affect. Disord. 217, 132–137. https://doi.org/10.1016/j.jad.2017.03.073.

Lan, M.J., Chhetry, B.T., Liston, C., Mann, J.J., Dubin, M., 2016. Transcranial magnetic stimulation of left dorsolateral prefrontal cortex induces brain morphological changes in regions associated with a treatment resistant major depressive episode: an exploratory analysis. Brain Stimul. 9, 577–583. https://doi.org/10.1016/j.brs.2016.02.011.

Lee, Y.J., Kim, S., Gwak, A.R., Kim, S.J., Kang, S.G., Na, K.S., et al., 2016. Decreased regional gray matter volume in suicide attempters compared to suicide non-attempters with major depressive disorders. Compr. Psychiatry 67, 59–65. https://doi.org/10.1016/j.comppsych.2016.02.013.

Li, L., Lu, B., Yan, C.G., 2020. Stability of dynamic functional architecture differs between brain networks and states. NeuroImage 216, 116230. https://doi.org/10.1016/j.neuroimage.2019.116230.

Li, Y., Li, Y., Wei, Q., Bai, T., Wang, K., Wang, J., et al., 2022. Mapping intrinsic functional network topological architecture in major depression disorder after electroconvulsive therapy. J. Affect. Disord. 311, 103–109. https://doi.org/10.1016/j.jad.2022.05.067.

Li, Y., Yu, X., Ma, Y., Su, J., Li, Y., Zhu, S., et al., 2023. Neural signatures of default mode network in major depression disorder after electroconvulsive therapy. Cereb. Cortex 33, 3840–3852. https://doi.org/10.1093/cercor/bhac311.

Liu, F., Hu, M., Wang, S., Guo, W., Zhao, J., Li, J., et al., 2012. Abnormal regional spontaneous neural activity in first-episode, treatment-naive patients with late-life depression: a resting-state fMRI study. Prog. Neuropsychopharmacol. Biol. Psychiatry 39, 326–331. https://doi.org/10.1016/j.pnpbp.2012.07.004.

Möller, H.J., 2008. Outcomes in major depressive disorder: the evolving concept of remission and its implications for treatment. World J. Biol. Psychiatry 9, 102–114. https://doi.org/10.1080/15622970801981606.

Mulders, P.C., van Eijndhoven, P.F., Schene, A.H., Beckmann, C.F., Tendolkar, I., 2015. Resting-state functional connectivity in major depressive disorder: a review. Neurosci. Biobehav. Rev. 56, 330–344. https://doi.org/10.1016/j.neubiorev.2015.07.014.

Nygren, A., Reutfors, J., Brandt, L., Bodén, R., Nordenskjöld, A., Tiger, M., 2023. Response to electroconvulsive therapy in treatment-resistant depression: nationwide observational follow-up study. BJPsych Open 9, e35. https://doi.org/10.1192/bjo.2023.5.

O'Doherty, J., Kringelbach, M.L., Rolls, E.T., Hornak, J., Andrews, C., 2001. Abstract reward and punishment representations in the human orbitofrontal cortex. Nat. Neurosci. 4, 95–102. https://doi.org/10.1038/82959.

Otte, C., Gold, S.M., Penninx, B.W., Pariante, C.M., Etkin, A., Fava, M., et al., 2016. Major depressive disorder. Nat. Rev. Dis. Primers. 2, 16065. https://doi.org/10.1038/nrdp.2016.65.

Pang, Y., Chen, H., Wang, Y., Long, Z., He, Z., Zhang, H., et al., 2018. Transdiagnostic and diagnosis-specific dynamic functional connectivity anchored in the right anterior insula in major depressive disorder and bipolar depression. Prog. Neuropsychopharmacol. Biol. Psychiatry 85, 7–15. https://doi.org/10.1016/j.pnpbp.2018.03.020.

Pang, Y., Wei, Q., Zhao, S., Li, N., Li, Z., Lu, F., et al., 2022. Enhanced default mode network functional connectivity links with electroconvulsive therapy response in major depressive disorder. J. Affect. Disord. 306, 47–54. https://doi.org/10.1016/j.jad.2022.03.035.

Phelps, E.A., 2004. Human emotion and memory: interactions of the amygdala and hippocampal complex. Curr. Opin. Neurobiol. 14, 198–202. https://doi.org/10.1016/j.conb.2004.03.015.

Preti, M.G., Bolton, T.A., Van De Ville, D., 2017. The dynamic functional connectome: state-of-the-art and perspectives. NeuroImage 160, 41–54. https://doi.org/10.1016/j.neuroimage.2016.12.061.

Raichle, M.E., MacLeod, A.M., Snyder, A.Z., Powers, W.J., Gusnard, D.A., Shulman, G.L., 2001. A default mode of brain function. Proc. Natl. Acad. Sci. U. S. A. 98, 676–682. https://doi.org/10.1073/pnas.98.2.676.

Ramirez, S., Liu, X., MacDonald, C.J., Moffa, A., Zhou, J., Redondo, R.L., et al., 2015. Activating positive memory engrams suppresses depression-like behaviour. Nature 522, 335–339. https://doi.org/10.1038/nature14514.

Roiser, J.P., Elliott, R., Sahakian, B.J., 2012. Cognitive mechanisms of treatment in depression. Neuropsychopharmacology 37, 117–136. https://doi.org/10.1038/npp.2011.183.

Rolls, E.T., 2017. The roles of the orbitofrontal cortex via the habenula in non-reward and depression, and in the responses of serotonin and dopamine neurons. Neurosci. Biobehav. Rev. 75, 331–334. https://doi.org/10.1016/j.neubiorev.2017.02.013.

Rolls, E.T., Cheng, W., Gilson, M., Qiu, J., Hu, Z., Ruan, H., et al., 2018. Effective connectivity in depression. Biol. Psychiatry Cogn. Neurosci. Neuroimaging 3, 187–197. https://doi.org/10.1016/j.bpsc.2017.10.004.

Rolls, E.T., Cheng, W., Feng, J., 2020. The orbitofrontal cortex: reward, emotion and depression. Brain Commun. 2, fcaa196. https://doi.org/10.1093/braincomms/fcaa196.

Schiller, C.E., Minkel, J., Smoski, M.J., Dichter, G.S., 2013. Remitted major depression is characterized by reduced prefrontal cortex reactivity to reward loss. J. Affect. Disord. 151, 756–762. https://doi.org/10.1016/j.jad.2013.06.016.

Sendi, M.S.E., Zendehrouh, E., Sui, J., Fu, Z., Zhi, D., Lv, L., et al., 2021. Abnormal dynamic functional network connectivity estimated from default mode network predicts symptom severity in major depressive disorder. Brain Connect. 11, 838–849. https://doi.org/10.1089/brain.2020.0748.

Shpokayte, M., McKissick, O., Guan, X., Yuan, B., Rahsepar, B., Fernandez, F.R., et al., 2022. Hippocampal cells segregate positive and negative engrams. Commun. Biol. 5, 1009. https://doi.org/10.1038/s42003-022-03906-8.

Stippl, A., Kirkgöze, F.N., Bajbouj, M., Grimm, S., 2020. Differential effects of electroconvulsive therapy in the treatment of major depressive disorder. Neuropsychobiology 79, 408–416. https://doi.org/10.1159/000505553.

Surguladze, S., Brammer, M.J., Keedwell, P., Giampietro, V., Young, A.W., Travis, M.J., et al., 2005. A differential pattern of neural response toward sad versus happy facial expressions in major depressive disorder. Biol. Psychiatry 57, 201–209. https://doi.org/10.1016/j.biopsych.2004.10.028.

Wang, J., Ji, Y., Li, X., He, Z., Wei, Q., Bai, T., et al., 2020. Improved and residual functional abnormalities in major depressive disorder after electroconvulsive therapy. Prog. Neuropsychopharmacol. Biol. Psychiatry 100, 109888. https://doi.org/10.1016/j.pnpbp.2020.109888.

Wang, L., Yu, L., Wu, F., Wu, H., Wang, J., 2019. Altered whole brain functional connectivity pattern homogeneity in medication-free major depressive disorder. J. Affect. Disord. 253, 18–25. https://doi.org/10.1016/j.jad.2019.04.040.

Wei, Q., Tian, Y., Yu, Y., Zhang, F., Hu, X., Dong, Y., et al., 2014. Modulation of interhemispheric functional coordination in electroconvulsive therapy for depression. Transl. Psychiatry 4, e453. https://doi.org/10.1038/tp.2014.101.

Wei, Q., Bai, T., Chen, Y., Ji, G., Hu, X., Xie, W., et al., 2018. The changes of functional connectivity strength in electroconvulsive therapy for depression: a longitudinal study. Front. Neurosci. 12, 661. https://doi.org/10.3389/fnins.2018.00661.

Wu, Y., Ji, Y., Bai, T., Wei, Q., Zu, M., Guo, Y., et al., 2022. Nodal degree changes induced by electroconvulsive therapy in major depressive disorder: evidence in two independent cohorts. J. Affect. Disord. 307, 46–52. https://doi.org/10.1016/j.jad.2022.03.045.

Yan, C.G., Wang, X.D., Zuo, X.N., Zang, Y.F., 2016. DPABI: Data Processing & Analysis for (Resting-State) Brain Imaging. Neuroinformatics 14, 339–351. https://doi.org/10.1007/s12021-016-9299-4.

Zhang, M., Wei, X., Li, S.Y., Liu, Q.M., Huang, X., Huang, X.B., et al., 2024. Sex differences in the antidepressant and neurocognitive effects of nonconvulsive electrotherapy in patients with treatment-refractory depression. Alpha Psychiatry. 25, 68–74. https://doi.org/10.5152/alphapsychiatry.2024.231402.

Zhang, X., Di, X., Lei, H., Yang, J., Xiao, J., Wang, X., et al., 2016. Imbalanced spontaneous brain activity in orbitofrontal-insular circuits in individuals with cognitive vulnerability to depression. J. Affect. Disord. 198, 56–63. https://doi.org/10.1016/j.jad.2016.03.001.

Zhao, P., Yan, R., Wang, X., Geng, J., Chattun, M.R., Wang, Q., et al., 2019. Reduced resting state neural activity in the right orbital part of middle frontal gyrus in anxious depression. Front. Psych. 10, 994. https://doi.org/10.3389/fpsyt.2019.00994.

Zhu, J., Zhang, S., Cai, H., Wang, C., Yu, Y., 2020. Common and distinct functional stability abnormalities across three major psychiatric disorders. NeuroImage Clinical. 27, 102352. https://doi.org/10.1016/j.nicl.2020.102352.